water

MDPI

Article

Discussion on the Choice of Decomposition Level for Wavelet Based Hydrological Time Series Modeling

Moyuan Yang [1,2], Yan-Fang Sang [1,*], Changming Liu [1] and Zhonggen Wang [1]

[1] Key Laboratory of Water Cycle and Related Land Surface Processes, Institute of Geographic Sciences and Natural Resources Research, Chinese Academy of Sciences, Beijing 100101, China; ymoyuan@163.com (M.Y.); liucm@igsnrr.ac.cn (C.L.); wangzg@igsnrr.ac.cn (Z.W.)

[2] University of Chinese Academy of Sciences, Beijing 100101, China

* Correspondence: sangyf@igsnrr.ac.cn; Tel.: +86-10-6488-9310

Academic Editors: Y. Jun Xu, Guangxin Zhang and Hongyan Li

Received: 1 March 2016; Accepted: 6 May 2016; Published: 12 May 2016

Abstract: The combination of wavelet analysis methods with data-driven models is a prevalent approach to conducting hydrological time series forecasting, but the results are affected by the accuracy of the wavelet decomposition of the series. The choice of decomposition level is one of the key factors for the wavelet decomposition. In this paper, the data of daily precipitation and streamflow time series measured in the upper reach of the Heihe River Basin in Northwest China were used as an example, and the influence of the decomposition level on wavelet-based hydrological time series forecasting was investigated. The true components of the precipitation series were identified, and the modeling results using 10 decomposition levels and two decomposition types were compared. The results affirmed that the wavelet-based modeling performance is sensitive to the choice of decomposition level, which is determined by the time series analyzed, but has no relation with the decomposition type used. The essence of the choice of decomposition level is to reveal the complex variability of hydrological time series under multi-temporal scales, and first knowing the true components of series could guide the choice of decomposition level. Through this study, the relationship among original series' characteristics, the choice of decomposition level, and the accuracy of wavelet-based hydrological time series forecasting can be more clearly understood, and it can be an improvement for wavelet-based data-driven modeling.

Keywords: wavelet analysis; decomposition level choice; temporal scale; hydrological time series forecasting; artificial neural network

1. Introduction

This paper mainly concerns the issue of hydrological time series forecasting (HTSF). It is done to understand the future hydrological regimes, then further guide various practical water activities, such as safe yield computations, hydrological and hydraulic designs, and water resources planning and management [1,2]. Currently, there have been a great number of relevant studies, and many methods and models, generally called data-driven models, can be used for the topic [3–5]. The basic idea of data-driven models is to use certain mathematical tools to describe correlations of hydrological variables, without requiring modeling of the internal structure of a watershed system [4,6,7]. An important and extensively accepted viewpoint about these models is that accurate identification of characteristics in hydrological time series is the basis of forecasting by the data-driven models [8,9]. However, many data-driven models cannot fully meet these needs. For instance, linear regression (LR) models provide only reasonable accuracy and suffer from the assumptions of stationarity and linearity [10]. Being different from LR models, the artificial neural network (ANN) models can learn

complicated nonlinear relationships and handle large amounts of dynamicity and noise concealed in datasets, but they cannot handle the nonstationarity of hydrological processes [11,12].

Wavelet analysis (WA) is a widely used method for hydrological time series analysis, because it can simultaneously elaborate the localized characteristics of nonstationary time series both in temporal and frequency domains [13–16]. Data pre-processing by wavelet analysis methods can give a relatively satisfactory ANN modeling result. Thereby, the combination of wavelet analysis with artificial neural network models (WA-ANN) has become a prevalent approach for HTSF, and various studies have indicated the advantages and effectiveness of the practice [17–20]. Theoretically, the WA-ANN model can handle the nonstationarity and nonlinearity of hydrological processes, but its effectiveness is greatly impacted by the result of the wavelet decomposition of the hydrological time series [21,22]. In the process of discrete wavelet decomposition, a key issue is the choice of decomposition level. It reflects the characteristics of hydrological processes under multi-temporal scales, and determines the accuracy of hydrological time series analysis.

When conducting wavelet decomposition for a WA-ANN model, present studies usually choose the decomposition level according to series length. For instance, Aussem *et al.* [23,24] used a formula $L = \log(N)$, where N is the series length, to choose a suitable decomposition level; Adamowski and Sun used the eight-level decomposition for developing wavelet-coupled neural network models [13]; Partal and Kişi employed decomposition at ten-level for developing a wavelet-coupled neuro-fuzzy model [25]; Kisi and Shiri used three decomposition levels for developing wavelet-based genetic programming and neuro-fuzzy models [26]; Shoaib *et al.* suggested the use of nine-level decomposition for the development of hybrid wavelet data-driven models [20,27,28]. From the above results we can easily find that those decomposition levels used for HTSF have large differences. In the authors' opinion, they would be unreasonable because of they do not considering the series' composition [29]. It is deduced here that there is limited understanding on the choice of decomposition level currently, and the impact of different decomposition types of series on wavelet-based modeling is not clearly known either.

In this paper, the main objective is to investigate the influence of decomposition level choice on wavelet-based hydrological time series forecasting. To achieve the goal, the method for discrete wavelet decomposition of series is firstly described. Then, daily precipitation and streamflow series measured in the upper reach of the Heihe River Basin are used as an example, and they are analyzed by the WA-ANN model with different decomposition levels. Through comparing and discussing the results, several understandings and suggestions for wavelet-based hydrological time series forecasting are given finally.

2. Methods

2.1. Study Area

The daily precipitation and streamflow series data in the upper reach of the Heihe River Basin are used in this study for discussing the influence of decomposition level choice on wavelet-based hydrological time series forecasting. The Heihe River Basin is the second-largest inland basin in Northwest China (Figure 1). The upper reach, with an area of 10,009 km^2, accounts for about 8% of the whole basin area, and the basin outlet is the Yingluoxia streamflow station.

2.2. Precipitation and Streamflow Data

The precipitation data measured at the Yeniugou and Qilian meteorological stations are used, and they are obtained from the China Meteorological Administration. Their arithmetic average values are used as the precipitation data for modeling. The streamflow data, measured at the Yingluoxia station, are mainly determined by precipitation processes, and can reflect the hydrological condition in the upper reach and the whole basin [30].

The daily precipitation and streamflow data series have the same length of 15 years (5479 days) measured from the 1990 to 2004. The first 10 years of the series data (3652 days, 67% of the whole data set) are used for calibration, and the remaining five years (1827 days, 33% of the whole data set) are used for verification. The statistical characters of these data sets are presented in Table 1, in which x_{mean}, x_{max}, x_{min}, C_v, and C_s denote the mathematical mean, maximum, minimum, coefficient of variation and coefficient of skewness, respectively. The precipitation and streamflow series in the calibration period show similar scattered variations as those in the verification period (*i.e.*, similar C_v values of 2.72 and 2.58, 1.11 and 0.96), but the former have higher positive skewness (*i.e.*, C_s = 4.97 compared with 4.13, 3.55 compared to 2.65). The precipitation data fall within the range of 0–34.70 mm in the calibration period, while those in the verification period fall within the range of 0–22.00 mm, being smaller than the former. The same results can be found in the streamflow data: the streamflow data fall within the range of 5.01–788.00 m^3/s in the calibration period, and those in the verification period are in the range of 4.08–504.00 m^3/s. According to the statistical characters, it is thought that extreme streamflow values in the verification period can be accurately modeled as long as a proper model is built by using the calibration data sets.

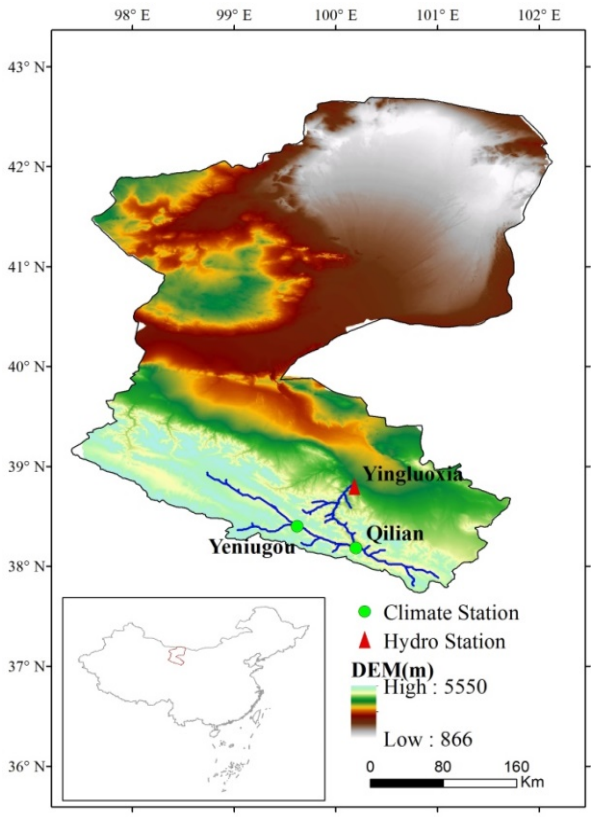

Figure 1. Location of the Heihe River Basin in China, and the hydrological station used in this study.

Table 1. Statistical characters of the precipitation and streamflow data sets used for the study.

Series Type	Period	Statistical Characters				
		x_{mean}	x_{max}	x_{min}	C_v	C_s
Precipitation (mm)	calibration	0.85	34.70	0	2.72	4.97
	verification	0.84	22.00	0	2.58	4.13
Streamflow (m^3/s)	calibration	50.20	788.00	5.01	1.11	3.55
	verification	49.37	503.00	4.08	0.96	2.65

2.3. Discrete Wavelet Transform and Modeling Design

Hydrological time series data are often measured as discrete signals. They are usually analyzed by the discrete wavelet transform (DWT) method in Equation (1) [31], mainly to identify true components and separate noise from original series:

$$W_f(j,k) = \int_{-\infty}^{+\infty} f(t)\psi_{j,k}{}^*(t)\ \mathrm{dt} \quad with \quad \psi_{j,k}(t) = {a_0}^{-j/2}\psi({a_0}^{-j}t - b_0k) \tag{1}$$

where $\psi(t)$ is the mother wavelet, $f(t)$ is the series analyzed, and t is an index representing time; a_0 and b_0 are constants, integer j is the decomposition level, and k is the time translation factor; $\psi^*(t)$ is the complex conjugate. In practice, the dyadic DWT in Equation (2) is used commonly by assigning $a_0 = 2$ and $b_0 = 1$ [32]:

$$W_f(j,k) = \int_{-\infty}^{+\infty} f(t)\psi_{j,k}{}^*(t)\ \mathrm{dt} \quad with \quad \psi_{j,k}(t) = 2^{-j/2}\psi(2^{-j}t - k) \tag{2}$$

In the dyadic DWT process, the first stage starts from the original signal, and the result includes two types of coefficients set as "approximation" and "detail" under each level. In each stage except the first one, only approximation coefficients are analyzed. More details of the mathematical foundations of dyadic DWT are thoroughly described in References [16,31]. The wavelet used for DWT must meet the regularity condition in Equation (3) with the regularity of order N:

$$\int_{-\infty}^{+\infty} t^k\psi(t)\mathrm{dt} = 0, \quad k = 1, \cdots, N-1 \tag{3}$$

Sub-signal $f_j(t)$ of the original series under the level j can be reconstructed by Equation (4), and their sum is the original series:

$$f_j(t) = \sum_k W_f(j,k)\psi^*(2^{-j}t - k) \tag{4}$$

Theoretically, the maximum decomposition level (M) can be calculated as: $M = \log_2(N)$, where N is the series length. When conducting a wavelet-based ANN model, it needs to determine the most suitable decomposition level from 1 to M. Along with the increase of decomposition level j, more sub-signals and detailed information of series at larger temporal scales would appear. More information may contribute to better performance of the model, but more input neutrals may reduce the computing efficiency and decrease the stability of the model. Therefore, it is important to select a suitable decomposition level for wavelet-neutral modeling.

In the study, we use the back propagation neural network (BPNN) model, which is commonly applied to hydrological time series modeling [4]. The input data of the BPNN model is precipitation data, and the output data is streamflow data. The number of neurons in the input layer is determined by the wavelet decomposition result of precipitation series, as described in the former section. The number of neurons in the hidden layer is determined by the 'trial and error' test, and one neuron in the output layer is the simulated streamflow series.

In the modeling practice, three main factors are considered: (1) the choice of decomposition level. Each of the levels from 1 to 10 is used to decompose the original series and conduct BPNN modeling, and 10 modeling results are compared; (2) two decomposition types. In order to analyze the influence of decomposition type on WA-BPNN modeling, two decomposition types are considered here. The first is called T-I: when using a certain decomposition level j, all the sub-signals D1, D2, ... , Dj, and Aj are used as the input data of the BPNN model. The other is called T-II: under a certain decomposition level j, the sum of sub-signals reconstructed by detailed coefficients (D1 + D2 + ... + Dj) and the sub-signal Aj are used as the input data of the BPNN model; (3) evaluation of modeling

result. Three indexes, *NSE* (Nash-Sutcliffe efficiency), *R* (correlation coefficient) and *AARE* (average absolute relative error), are used here to evaluate the accuracy of forecasting results. Their equations are described as:

$$NSE = 1 - \frac{\sum_{i=1}^{n} \left(Y_i^{obs} - Y_i^{sim}\right)^2}{\sum_{i=1}^{n} \left(Y_i^{obs} - Y_{mean}^{obs}\right)^2} \tag{5}$$

$$R = \frac{\sum_{i=1}^{n} (Y_i^{obs} - Y_{mean}^{obs}) \cdot (Y_i^{sim} - Y_{mean}^{sim})}{\sqrt{\sum_{i=1}^{n} (Y_i^{obs} - Y_{mean}^{obs})^2 \cdot \sum_{i=1}^{n} (Y_i^{sim} - Y_{mean}^{sim})^2}} \tag{6}$$

$$AARE = \frac{1}{n} \sum_{i=1}^{n} \left| \frac{Y_i^{sim} - Y_i^{obs}}{Y_i^{obs}} \right| \times 100\% \tag{7}$$

in which Y_i^{bs} and Y_i^{sim} denote the observation and simulated series, and $Y_{mean}{}^{bs}$ and $Y_{mean}{}^{sim}$ denote their mean values, respectively; n is the series length. The *NSE* coefficient is widely used for assessment of the model's performance [33]. *R* is an index commonly used to describe the correlation of two series. *AARE* can measure the error between the observation and simulated data [34]. In general, high *NSE* and *R* values and small *AARE* values indicate good modeling performance.

Following the "trial and error" test result, the number of neurons in the hidden layer is determined as five. The correlation analysis method is used to determine the time delay of the daily precipitation and streamflow data. In Figure 2, the lag-1 correlation coefficient between the precipitation and streamflow series is 0.62, being bigger than the lag-0 correlation coefficient of 0.47, so the time delay is determined as one day, meaning the streamflow value in a certain day is forecasted by using the daily precipitation data in the same and previous days.

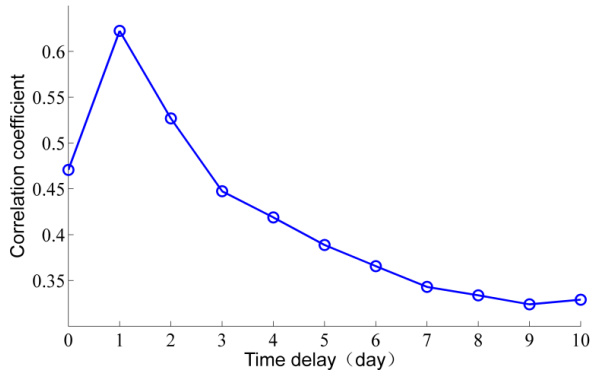

Figure 2. Correlation coefficients of the daily precipitation and streamflow series under different time delays.

3. Results

3.1. Wavelet Decomposition of Precipitation

The length of the precipitation series in the verification period is 1827, so the maximum decomposition level 10 (*i.e.*, $\log_2 1827$) is used here. By considering both the deterministic characteristics of the series and the mathematical properties of the wavelets, we used the method in Reference [35] and chose the "db3" mother wavelet to analyze the precipitation series in the verification and calibration periods. They are decomposed into 11 sub-signals by the discrete wavelet decomposition method. The sub-signals of the original series under "D" levels are reconstructed by detailed

wavelet coefficients, and the sub-signal under the "A" level is reconstructed by approximate wavelet coefficients, and it is usually the mean or trend of the original series. The method of significance testing of DWT proposed by Sang [35] is used here to judge the sub-signals of series under each level belonging to true components or noise.

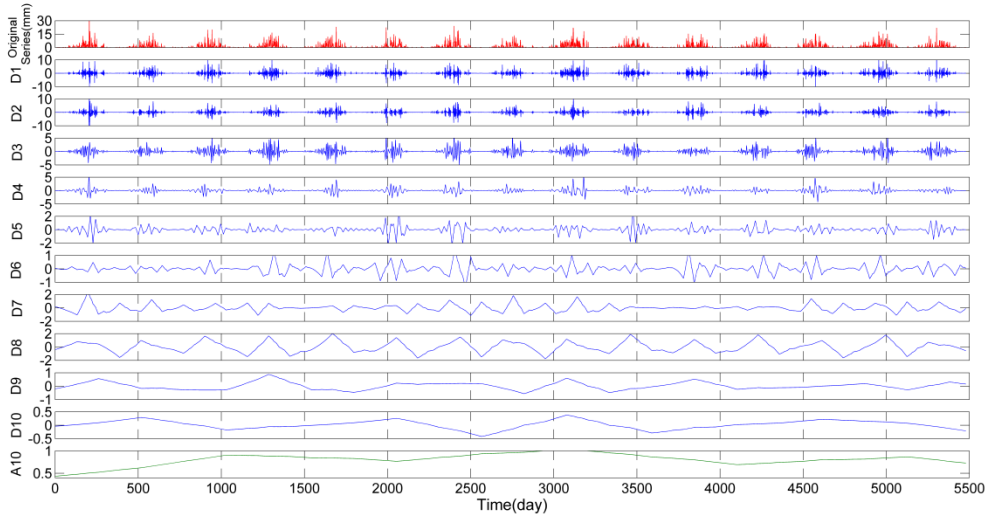

Figure 3. Results of discrete wavelet decomposition of precipitation series under each level.

The decomposition results of precipitation by the "db3" mother wavelet under level 10 are shown in Figure 3, and there are 10 detailed sub-signals and 1 approximate sub-signal. The detail components represent the two-day periodicity (D1), four-day periodicity (D2), eight-day periodicity (D3), . . . , and 2^{10}-day periodicity (D10). A10 represents the approximation component at the 10-level of decomposition. Lower detail levels have higher frequencies, which represent the rapidly changing component of the dataset, whereas the higher detail levels have lower frequencies, which represent the slowly changing component of the dataset. The approximation components (A10) represent the slowest changing component of the dataset (including the trend).

The energy function of the precipitation and streamflow series is compared with the referenced energy function with a 95% confidence interval, and the results are shown in Figure 4. For the sub-signals of the precipitation series, the energies of sub-signals under D3, D4, D7 and D8 are obviously above the 95% confidence interval, thus they are thought of as the true components, and other sub-signals are thought as noise.

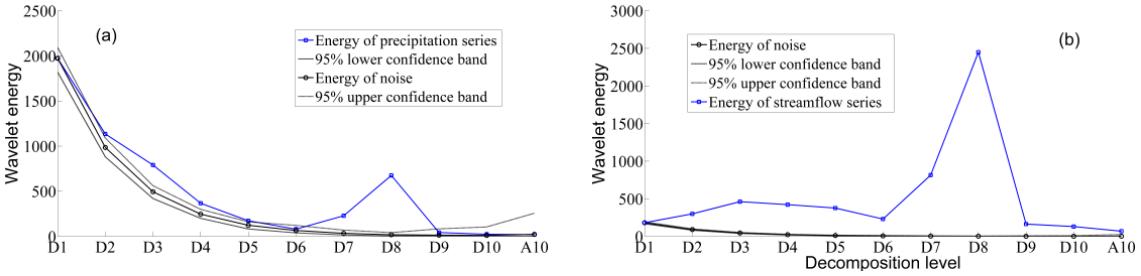

Figure 4. Energy functions of the precipitation (**a**); and streamflow (**b**) series and the reference energy function with 95% confidence interval.

3.2. Forecasting by Different Decomposition Levels

The modeling results of WA-BPNN models by the T-I type are shown in Table 2 and Figure 5. On the whole, the modeling performance becomes better along with the increase of the decomposition

level before level 6, but is stable afterwards. To be specific, the *NSE* value in the calibration period rises rapidly from 0.65 to 0.82 before level 6, and becomes stable afterwards, with the value of 0.82–0.83. Being similar to the calibration period, the *NSE* value in the verification period rises rapidly from 0.51 to 0.81 before level 6, and then becomes stable, with the value of 0.80–0.82. The same variations can be found in the *R* results. In the calibration and verification periods, the *R* value rises rapidly from 0.67 to 0.91 before level 6, and then becomes stable, with the value of 0.91. In the calibration and verification periods, the *AARE* value decreases rapidly from 0.43 to 0.25 before level 6, and then becomes stable, with the value of 0.25.

Table 2. Modeling results of WA-ANN models when using the T-I decomposition type.

Period	Index	Mode Name *										
		T-I-0	**T-I-1**	**T-I-2**	**T-I-3**	**T-I-4**	**T-I-5**	**T-I-6**	**T-I-7**	**T-I-8**	**T-I-9**	**T-I-10**
Calibration	*NSE*	0.54	0.65	0.70	0.77	0.80	0.81	0.82	0.83	0.83	0.83	0.82
	R	0.74	0.81	0.84	0.88	0.89	0.91	0.91	0.91	0.91	0.91	0.91
	AARE	0.41	0.36	0.32	0.27	0.26	0.25	0.25	0.24	0.24	0.24	0.24
Verification	*NSE*	0.43	0.51	0.60	0.70	0.76	0.79	0.81	0.82	0.81	0.80	0.80
	R	0.67	0.73	0.78	0.84	0.87	0.89	0.91	0.91	0.91	0.90	0.90
	AARE	0.43	0.40	0.35	0.30	0.27	0.25	0.24	0.23	0.24	0.25	0.25

* T-I-0 is the original precipitation series without any process, and T-I-*n* is the T-I type under the level *n*.

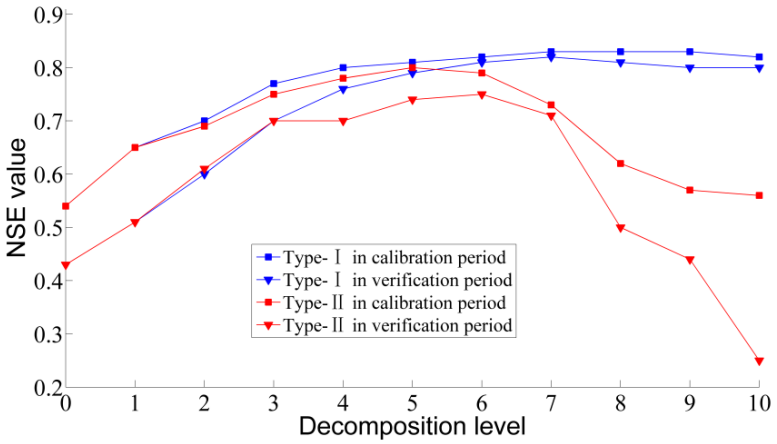

Figure 5. NSE values of the WA-ANN modeling results by two decomposition types under 10 decomposition levels. The result under the decomposition level 0 is obtained by using original series.

Table 3. Modeling results of WA-ANN models when using the T-II decomposition type.

Period	Index	Mode Name *										
		T-II-0	**T-II-1**	**T-II-2**	**T-II-3**	**T-II-4**	**T-II-5**	**T-II-6**	**T-II-7**	**T-II-8**	**T-II-9**	**T-II-10**
Calibration	*NSE*	0.54	0.65	0.69	0.75	0.78	0.80	0.79	0.73	0.62	0.57	0.56
	R	0.74	0.81	0.83	0.87	0.88	0.89	0.89	0.85	0.79	0.76	0.75
	AARE	0.41	0.36	0.34	0.29	0.27	0.26	0.26	0.31	0.36	0.39	0.40
Verification	*NSE*	0.43	0.51	0.61	0.70	0.70	0.74	0.75	0.71	0.50	0.44	0.25
	R	0.67	0.73	0.78	0.85	0.84	0.86	0.87	0.84	0.72	0.67	0.58
	AARE	0.43	0.40	0.35	0.29	0.31	0.28	0.29	0.32	0.39	0.45	0.40

* T-II-0 is the original precipitation series without any process, and T-II-*n* is the T-II type under the decomposition level *n*.

The modeling results by the T-II type are shown in Table 3 and Figure 5. On the whole, with the increase of the decomposition level, the modeling efficiency also shows a trend of increase at first and

a decrease later on. To be specific, the *NSE* values in the calibration period rise rapidly from 0.65 to 0.80 before level 6, and decrease from 0.73 to 0.56 afterwards. Similar to the calibration period, the *NSE* values in the verification period rise rapidly from 0.51 to 0.75 before level 6, and then drop rapidly from 0.71 to 0.25. The same change process can be found in the *R* value results. In the calibration period the *R* values rise from 0.74 to 0.89 before level 6, and then decrease to 0.75 under level 10. In the verification period the *R* values rise from 0.67 to 0.87 before level 6, and then decrease to 0.58 under level 10. Both in the calibration and verification periods, the *AARE* values decrease rapidly from 0.43 to about 0.26 before level 6, and then rise to 0.40 under level 10.

4. Discussion

The wavelet analysis method can identify deterministic components of hydrological time series and provide a reliably physical basis for a single artificial intelligence model, which is a main defect of data-driven models. Following the above results (Tables 2 and 3 and Figure 5), we can find that the modeling performance under decomposition level 6 is better than others, no matter which decomposition type is used. Therefore, decomposition level 6 is chosen as the best one for the modeling practice in this case. From the significance testing result of DWT in Figure 4, we can find that the sub-signals of the precipitation series before D6 (D1, D2, ... , D6) are more likely to be composed of noise, and the sub-signals after D7 (D7, D8, ... , D10 and A10) are mainly true components in the original series which reflect the annual and inter-annual periodicities and trends of the precipitation process. The first important understanding obtained from the above results is that a proper decomposition level should be carefully chosen when doing wavelet-based modeling, because it determines the accuracy of the wavelet decomposition result of a series, and further has great influence on the data-driven modeling practice.

Comparison of the results in Tables 2 and 3 shows that decomposition level 6 can distinguish the true components and noise in the original precipitation series, and it can accurately identify the deterministic characteristics of the series. For the T-I decomposition type, the true components and noise in the daily precipitation series can be distinguished when using decomposition level 6 or higher, so the modeling accuracy becomes stable after level 6. For the T-II decomposition type, when using decomposition levels from 7 to 10, some true components are mixed with noise, and they are not accurately distinguished. In the situation, if all of them are still used as the input data of the wavelet-aided BPNN model, the modeling accuracy both in the calibration and verification periods becomes worse compared with those in the T-I decomposition type. Here, the second important understanding obtained from the results is that the true components and noise in the original series should be accurately separated before wavelet-based modeling practice.

When using the conventional method [23,24], the proper decomposition level is computed as 3 (*i.e.*, $\log_{10}(5479)$) for the study. From Figure 5 we can find that both in the calibration and verification processes, the modeling results under level 3 are much worse than those under level 6, because the annual and inter-annual variability of precipitation series cannot be clearly identified when using decomposition level 3. Therefore, the third important understanding gained from the above results is that the choice of a suitable decomposition level should meet the need of the accurate identification of series' characteristics and composition, which is the basis of wavelet-based modeling. To be specific, the choice of decomposition level should be based on the characteristics of the analyzed series, but should not consider the series length or other factors, and unreasonable decomposition of the original series would cause bad wavelet-aided modeling performance.

As a result, the choice of decomposition level is an important issue in wavelet analysis and modeling. Presently, there have been a great number of studies on wavelet analysis of hydrological time series. For example, Sang established a reference energy function for discrete wavelet analysis, and proposed a practical guide to discrete wavelet decomposition of series [35]. It is used to choose an appropriate wavelet according to the relationship of the statistical characters among the original series, de-noised series and removed noise, to choose a proper decomposition level by analyzing

the difference between the energy function of the analyzed series and the reference energy function, and then to identify deterministic components by conducting significance testing of DWT. The guide is based on the hydrological time series itself, and it is recommended here for wavelet-based data pre-processing and modeling. From the study we think that the understanding about the issue of decomposition level choice should be improved, and specifically for long-term hydrological time series modeling, the decomposition level should at least reflect the inter-annual periodicities and decadal variability of hydrological time series, which are important deterministic characteristics of hydrological processes. It can be a principle and basis for the choice of decomposition level.

5. Conclusions

In this paper, by analyzing the daily precipitation and streamflow data in the upper reach of the Heihe River Basin, the influence of the decomposition level choice on WA-ANN modeling performance was investigated. By summing up the results, two important understandings about the issue are obtained: (1) no matter which decomposition type is used, the choice of decomposition level has a strong influence on the WA-ANN modeling performance, reflecting the importance of accurate wavelet-based data pre-processing practice; (2) the best decomposition level selected from the results is just the same for two decomposition types, which means that the choice of a suitable decomposition level is determined by the time series analyzed, but has no relation to the decomposition type used. By comprehensive analysis, it can be found that the essence of decomposition level choice is to reveal the complex variability of the hydrological process under multi-temporal scales. When using the method recommended in the study, we can choose an appropriate decomposition level by analyzing the difference between the energy function of the analyzed series and the reference energy function, and then identify deterministic components by conducting significance testing of DWT.

In the future, other key issues about the wavelet analysis, such as the choice of mother wavelet and the uncertainty analysis, should be further studied to improve wavelet-based models. Furthermore, more hydrological data examples should be analyzed to certify the reliability of the understanding about the issue of decomposition level choice obtained from this paper.

Acknowledgments: The authors gratefully acknowledged the helpful comments and suggestions on the manuscript given by the Editor and the anonymous reviewers. This project was financially supported by the key project of the National Natural Science Foundation of China (No. 41330529, 41201036), and the Program for the "Bingwei" Excellent Talents from the Institute of Geographic Sciences and Natural Resources Research, Chinese Academy of Sciences.

Author Contributions: Moyuan Yang did the detailed work and wrote the paper; Yan-Fang Sang provided the method and guided the entire study; Changming Liu contributed to the discussion part; Zhonggen Wang analyzed the data.

Conflicts of Interest: The authors declare no conflict of interest.

References

1. Cheng, C.T.; Xie, J.X.; Chau, K.W.; Layeghifard, M. A new indirect multi-step-ahead prediction model for a long-term hydrologic prediction. *J. Hydrol.* **2008**, *361*, 118–130. [CrossRef]
2. Tiwari, M.K.; Chatterjee, C. Uncertainty assessment and ensemble flood forecasting using bootstrap based artificial neural networks (banns). *J. Hydrol.* **2010**, *382*, 20–33. [CrossRef]
3. Alvisi, S.; Franchini, M. Fuzzy neural networks for water level and discharge forecasting with uncertainty. *Environ. Model. Softw.* **2011**, *26*, 523–537. [CrossRef]
4. Jain, A.; Kumar, A.M. Hybrid neural network models for hydrological time series forecasting. *Appl. Soft. Comput.* **2007**, *7*, 585–592. [CrossRef]
5. Nourani, V.; Alami, M.T.; Aminfar, M.H. A combined neural-wavelet model for prediction of ligvanchai watershed precipitation. *Eng. Appl. Artif. Intel.* **2009**, *22*, 466–472. [CrossRef]
6. Kisi, O. Wavelet regression model for short-term streamflow forecasting. *J. Hydrol.* **2010**, *389*, 344–353. [CrossRef]

7. Kişi, Ö. Wavelet regression model as an alternative to neural networks for monthly streamflow forecasting. *Hydrol. Process.* **2009**, *23*, 3583–3597.
8. Sang, Y.F. Improved wavelet modeling framework for hydrological time series forecasting. *Water Resour. Manag.* **2013**, *27*, 2807–2821. [CrossRef]
9. Nourani, V.; Baghanam, A.H.; Adamowski, J.; Kisi, O. Applications of hybrid wavelet–artificial intelligence models in hydrology: A review. *J. Hydrol.* **2014**, *514*, 358–377. [CrossRef]
10. Kwon, H.H.; Lall, U.; Khalil, A.F. Stochastic simulation model for nonstationary time series using an autoregressive wavelet decomposition: Applications to rainfall and temperature. *Water Resour. Res.* **2007**, *43*. [CrossRef]
11. Cannas, B.; Fanni, A.; See, L.; Sias, G. Data preprocessing for river flow forecasting using neural networks: Wavelet transforms and data partitioning. *Phys. Chem. Earth.* **2006**, *31*, 1164–1171. [CrossRef]
12. Rajurkar, M.; Kothyari, U.; Chaube, U. Modeling of the daily rainfall-runoff relationship with artificial neural network. *J. Hydrol.* **2004**, *285*, 96–113. [CrossRef]
13. Adamowski, J.; Sun, K. Development of a coupled wavelet transform and neural network method for flow forecasting of non-perennial rivers in semi-arid watersheds. *J. Hydrol.* **2010**, *390*, 85–91. [CrossRef]
14. Grossmann, A.; Morlet, J. Decomposition of hardy functions into square integrable wavelets of constant shape. *SIAM J. Math. Ana.* **1984**, *15*, 723–736. [CrossRef]
15. Maheswaran, R.; Khosa, R. Wavelet–volterra coupled model for monthly stream flow forecasting. *J. Hydrol.* **2012**, *450*, 320–335. [CrossRef]
16. Torrence, C.; Compo, G.P. A practical guide to wavelet analysis. *B. Am. Meteorol. Soc.* **1998**, *79*, 61–78. [CrossRef]
17. Adamowski, J.F. River flow forecasting using wavelet and cross-wavelet transform models. *Hydrol. Process.* **2008**, *22*, 4877–4891. [CrossRef]
18. Kişi, Ö. Neural network and wavelet conjunction model for modelling monthly level fluctuations in Turkey. *Hydrol. Process.* **2009**, *23*, 2081–2092.
19. Nourani, V.; Mogaddam, A.A.; Nadiri, A.O. An ann-based model for spatiotemporal groundwater level forecasting. *Hydrol. Process.* **2008**, *22*, 5054–5066. [CrossRef]
20. Shoaib, M.; Shamseldin, A.Y.; Melville, B.W. Comparative study of different wavelet based neural network models for rainfall-runoff modeling. *J. Hydrol.* **2014**, *515*, 47–58. [CrossRef]
21. Tiwari, M.K.; Chatterjee, C. Development of an accurate and reliable hourly flood forecasting model using wavelet-bootstrap-ANN (WBANN) hybrid approach. *J. Hydrol.* **2010**, *394*, 458–470. [CrossRef]
22. Zhou, H.C.; Peng, Y.; Liang, G.H. The research of monthly discharge predictor-corrector model based on wavelet decomposition. *Water Resour. Manag.* **2008**, *22*, 217–227. [CrossRef]
23. Nourani, V.; Komasi, M.; Mano, A. A multivariate ann-wavelet approach for rainfall-runoff modeling. *Water Resour. Manag.* **2009**, *23*, 2877–2894. [CrossRef]
24. Aussem, A.; Campbell, J.; Murtagh, F. Wavelet-based feature extraction and decomposition strategies for financial forecasting. *J. Comput. Intell. Finan.* **1998**, *6*, 5–12.
25. Partal, T.; Kişi, Ö. Wavelet and neuro-fuzzy conjunction model for precipitation forecasting. *J. Hydrol.* **2007**, *342*, 199–212. [CrossRef]
26. Kisi, O.; Shiri, J. Precipitation forecasting using wavelet-genetic programming and wavelet-neuro-fuzzy conjunction models. *Water Resour. Manag.* **2011**, *25*, 3135–3152. [CrossRef]
27. Shoaib, M.; Shamseldin, A.Y.; Melville, B.W.; Khan, M.M. Hybrid wavelet neuro-fuzzy approach for rainfall-runoff modeling. *J. Comput. Civil Eng.* **2014**, *30*, 04014125. [CrossRef]
28. Shoaib, M.; Shamseldin, A.Y.; Melville, B.W.; Khan, M.M. Runoff forecasting using hybrid Wavelet Gene Expression Programming (WGEP) approach. *J. Hydrol.* **2015**, *527*, 326–344. [CrossRef]
29. Nourani, V.; Kisi, Ö.; Komasi, M. Two hybrid artificial intelligence approaches for modeling rainfall-runoff process. *J. Hydrol.* **2011**, *402*, 41–59. [CrossRef]
30. Li, Z.; Xu, Z.; Shao, Q.; Yang, J. Parameter estimation and uncertainty analysis of swat model in upper reaches of the heihe river basin. *Hydrol. Process.* **2009**, *23*, 2744–2753. [CrossRef]
31. Percival, D.B.; Walden, A.T. *Wavelet Methods for Time Series Analysis*; Cambridge University Press: Cambridge, UK, 2006.
32. Daubechies, I. *Ten Lectures on Wavelets*; Society for industrial and applied Mathematics: Philadelphia, PA, USA, 1992.

33. Nash, J.E.; Sutcliffe, J.V. River flow forecasting through conceptual models part I—A discussion of principles. *J. Hydrol.* **1970**, *10*, 282–290. [CrossRef]
34. Jain, A.; Srinivasulu, S. Development of effective and efficient rainfall-runoff models using integration of deterministic, real-coded genetic algorithms and artificial neural network techniques. *Water Resour. Res.* **2004**, *40*, W04302. [CrossRef]
35. Sang, Y.F. A practical guide to discrete wavelet decomposition of hydrologic time series. *Water Resour. Manag.* **2012**, *26*, 3345–3365. [CrossRef]